PROCEEDINGS OF SCIENCE

Shedding light on low-mass subhalo survival and annihilation luminosity with numerical simulations

Alejandra Aguirre-Santaella,[a,b,*] **Miguel A. Sánchez-Conde,**[a,b] **Go Ogiya,**[c] **Jens Stücker**[d] **and Raul E. Angulo**[d,e]

[a] *Instituto de Física Teórica UAM-CSIC, Universidad Autónoma de Madrid, C/ Nicolás Cabrera, 13-15, 28049 Madrid, Spain*

[b] *Departamento de Física Teórica, M-15, Universidad Autónoma de Madrid, E-28049 Madrid, Spain*

[c] *Institute for Astronomy, School of Physics, Zhejiang University, Hangzhou 310027, China*

[d] *Donostia International Physics Center (DIPC), Manuel Lardizabal Ibilbidea, 4, 20018 Donostia, Gipuzkoa, Spain*

[e] *IKERBASQUE, Basque Foundation for Science, 48013, Bilbao, Spain*

E-mail: alejandra.aguirre@uam.es, miguel.sanchezconde@uam.es

In this work, we carry out a suite of specially designed numerical simulations to shed light on dark matter (DM) subhalo survival at mass scales relevant for gamma-ray DM searches, a topic subject to intense debate nowadays. We have employed an improved version of DASH, a GPU N-body code, to study the evolution of low-mass subhaloes inside a Milky-Way-like halo with unprecedented accuracy, reaching solar-mass and sub-parsec resolution. We simulate subhaloes with varying mass, concentration, and orbital properties, and consider the effect of baryons in the host. We analyse the evolution of the bound mass fraction and annihilation luminosity, finding that most subhaloes survive until present, yet losing in some cases more than 99 per cent of their initial mass. Baryons induce a much greater mass-loss, especially when the subhalo orbit is more parallel to the Galactic disc. Many of these subhaloes cross the solar Galactocentric radius, making it easier to detect their annihilation fluxes from Earth. We find subhaloes orbiting a DM-only halo with a pericentre in the solar vicinity to lose 70–90% of their initial annihilation luminosity at present, which increases up to 99% when including baryons. We find a strong relation between subhalo's mass-loss and the effective tidal field at pericentre. Indeed, much of the dependence on all considered parameters can be explained through this single parameter. In addition to shedding light on the survival of low-mass Galactic subhaloes, our results can provide detailed predictions that will aid current and future quests for the nature of DM.

38th International Cosmic Ray Conference (ICRC2023)
26 July - 3 August, 2023
Nagoya, Japan

*Speaker

© Copyright owned by the author(s) under the terms of the Creative Commons Attribution-NonCommercial-NoDerivatives 4.0 International License (CC BY-NC-ND 4.0).

PoS(ICRC2023)004

1. Introduction

There is strong evidence to believe that there should exist something else apart from the matter we are able to observe in the Universe. Indeed, there are completely independent cosmological and astrophysical observations that point that, if our theory of gravity is correct, the mass of the matter we can detect electromagnetically is not enough to explain certain phenomena, whilst adding a new matter component, dark matter (DM), they are possible [1, 2].

Despite our efforts, the nature of the DM is yet unknown. There are three main different yet complementary methods to look for DM: direct production (using collider experiments in particle accelerators), direct detection (that look for traces of interactions between DM and baryonic matter at the laboratory) and indirect detection [3]. The indirect detection method aims to observe the radiation (gamma-rays and neutrinos) and antimatter (e.g. positrons) produced by DM annihilation or decay into Standard Model particles which could be detected through spatial or terrestrial observatories, such as Cherenkov Telescopes and *Fermi*-LAT [4]. A detection of these annihilation products might give a hint about DM properties [5]. Moreover, all evidence we have on DM is astrophysical as of today, thus indirect searches are the only ones that have the potential not only to make the necessary connection between the nature of the DM and the astrophysical observations, but also to provide direct information about the actual DM distribution in the Universe.

Standard ΛCDM cosmology predicts a hierarchical procedure for structure formation, with *haloes* which merge forming larger structures [6]. As a consequence, there is a huge amount of low-mass subhaloes, both dwarf galaxies and dark satellites, inside larger haloes like our galaxy, the Milky Way (MW).

Using cosmological N-body simulations makes it possible to study the formation of cold DM haloes and their substructure in the non-linear regime in great detail [7–9]. Nonetheless, basic properties of subhaloes such as their abundance, distribution and structure remain unclear for the less massive subhaloes due to the limited resolution in the simulations [10]. Finite numerical resolution also implies that at least some subhaloes will be artificially destroyed in simulations.

Indeed, it is unclear whether small subhaloes will survive the strong tidal forces within their hosts since their accretion times to present [11, 12]. Some authors claim that almost all subhalo disruption is of numerical origin and a bound remnant should always survive [11, 13, 14], while other studies suggest that the abundance of small subhaloes is severely reduced due to the effect of tidal forces and of other dynamical agents such as the presence of baryonic material [15–17].

Both subhaloes hosting dwarf satellite galaxies and dark satellites are known to be excellent targets for gamma-ray DM searches since some of them may be close enough to yield large DM annihilation fluxes at Earth [18]. Also, the DM-annihilation flux is related to the annihilation luminosity, which is proportional to the DM density squared. Thus, the clumpy distribution of subhaloes will considerably boost the total DM annihilation in their host haloes.

Here, we carry out a suite of specially-designed numerical simulations to shed further light on subhalo survival at all mass scales relevant for DM searches. Specifically, we have employed the DASH[1] simulation code [13] to study the evolution of subhaloes inside a MW-like halo with unprecedented accuracy. It simulates the dynamical evolution of subhaloes with the N-body

[1]While DASH is actually the name of the simulation library, we are calling the code used in our work this way for simplicity.

PoS(ICRC2023)004

method and analytically describes the gravitational potential of the host. In this way, computational resources are focused on a single subhalo. More precisely, we will throw a subhalo inside the host and follow its dynamics under different initial configurations such as concentrations, masses, orbital parameters and accretion redshifts. We will also analyze the effect of taking into account the baryonic disk in the host potential.

Our work is expected to be particularly relevant for DM searches which, indeed, represent one of our ultimate goals. On one hand, we may get significantly larger DM fluxes at Earth from astrophysical objects, such as entire galaxies or galaxy clusters, if we can prove that a significant amount of small subhaloes survive the tidal forces they undergo since their accretion times till present time. On the other, some of the surviving, tiny subhaloes closest to Earth would be excellent DM targets by themselves.

2. Simulation Model

We simulate the dynamical evolution of a DM subhalo orbiting within the MW potential, which consists of a DM host halo, stellar and gas disks, and a bulge. The subhalo is modelled as an N-body system, while a time-evolving analytical potential is employed to model the MW. In this Section, we describe our simulation model and parameter choice.

2.1 Subhalo

In this study, we consider subhaloes that do not host any stars, and thus they purely consist of DM. Due to the cosmic UV background radiation, star formation in haloes with a virial mass $\lesssim 10^8$ $M_\odot$ is suppressed and the gas within such haloes evaporates. While we employ the subhalo mass of $m_{\rm sub} = 10^6$ $M_\odot$ in our main simulations, the simulation results can be, in principle, scaled down to arbitrarily small halo masses [14]. Specifically, in this work we have tested subhalo masses down to 1 $M_\odot$ (see Section 3.1.2).

We suppose that prior to accretion, the subhalo is spherical and follows the Navarro-Frenk-While (NFW) density profile [19],

$$\rho(r) = 4\rho_{\rm s}(r/r_{\rm s})^{-1}(1 + r/r_{\rm s})^{-2}, \tag{1}$$

where r represents the distance from the centre of the halo, and $\rho_{\rm s}$ and $r_{\rm s}$ are the scale density and radius, respectively. The pair of the structural parameters ($\rho_{\rm s}$ and $r_{\rm s}$) can be derived from another pair of parameters, and we employ a pair of the virial mass, M_{200}, and the halo concentration, c, to specify the internal structure of the DM halo. The virial mass of the halo is given as

$$M_{200} \equiv (800\pi/3)\rho_{\rm crit}(z)r_{200}^3, \tag{2}$$

where $\rho_{\rm crit}(z)$ is the critical density of the Universe at redshift z, and r_{200} is the virial radius of the halo within which the mean density corresponds to $200\rho_{\rm crit}(z)$. The halo concentration is defined as $c \equiv r_{200}/r_{\rm s}$. For more details on the subhalo particle distribution, refer to [20].

PoS(ICRC2023)004

2.2 The host potential

The host potential is composed of a spherical DM host halo and the MW galaxy that consists of stellar and gas disks and a spherical bulge. The structural parameters of each component evolve with time, based on the empirical relations from cosmological simulations and observations. We input the masses of the DM halo and baryons and parameters introducing their spatial scales at $z = 0$. For more details on the DM and baryonic potentials, refer to [20].

2.3 Subhalo orbit

We take only the potential of the spherical DM host halo into account to set the initial subhalo orbit in the host-centric frame (baryon potentials are ignored in setting the initial subhalo orbit). An advantage of this scheme is that the initial velocity vector of the subhalo is identical when fixing the orbital parameters. The subhalo orbit is characterised with the orbital energy, the angular momentum, and the orbital plane. We employ the following three parameters in this study. The first one describes the orbital energy of the subhalo orbit in the host-centric frame,

$$x_{\rm c} \equiv r_{\rm c}(E)/r_{200,\rm host}(z_{\rm acc}), \tag{3}$$

where $r_{\rm c}(E)$ and $r_{200,\rm host}(z_{\rm acc})$ are the radius of a circular orbit of the orbital energy, E, and the virial radius of the host halo at the accretion redshift of the subhalo, $z_{\rm acc}$, respectively. The second one controls the angular momentum of the orbit,

$$\eta \equiv L/L_{\rm c}(E), \tag{4}$$

where L and $L_{\rm c}(E)$ are the actual angular momentum of the subhalo orbit and the angular momentum of the circular orbit of the energy, E. The third parameter is the inclination angle with respect to the galactic plane, θ.

2.4 Numerical techniques

For N-body computation, we use a code that adopts an oct-tree algorithm [21] and is accelerated with Graphics Processing Units [22]. The gravitational potential field of particles is smoothed with a force softening of $\varepsilon = 0.0003\, r_{200,\rm sub}$ and with a force accuracy parameter of $\alpha = 0.01$. The position and velocity vectors of particles are updated with the second-order Leapfrog scheme in each N-body iteration. The centre of the subhalo and its bulk velocity in the host-centric coordinate system is tracked with the scheme outlined in [11]. The evolution of the mass bound to the subhalo is also computed. Only bound particles are considered in drawing the spherically averaged density profile of the subhalo.

2.5 Parameter choices

The high numerical accuracy will enable us to study with great detail subhalo survival and its impact in gamma-ray DM searches using the set of parameters that suit best our purposes. We simulate subhaloes with varying mass, concentration, and orbital properties, thus covering the different properties expected in a realistic cosmological scenario. We use six parameters to simulate the subhalo [see 20, for more details]: The initial subhalo mass, $m_{\rm sub}$; the subhalo accretion redshift,

PoS(ICRC2023)004

Table 1: Set of parameters used in this work, described in Section 2.5. First column: fiducial parameters. Second column: studied range of each parameter in the full suite.

	fiducial	suite
$m_{\rm sub}[{\rm M}_\odot]$	10^6	$[1, 10^9]$
$z_{\rm acc}$	2	$[1, 4]$
c	10	$[5, 50]$
η	0.3	$[0.1, 0.8]$
$x_{\rm c}$	1.2	$[0.8, 1.6]$
θ [deg]	45	$[0, 90]$

Table 2: Examples of mass resolution, mean inter-particle distance and softening length for some subhalo masses and number of particles used in this work. All cases assume $z_{\rm acc} = 2$.

$m_{\rm sub}[{\rm M}_\odot]$	N	$m_{\rm resol}[{\rm M}_\odot]$	$d_{\rm ip}$ [pc]	ε [pc]
10^6	2^{18}	3.81	0.16	0.304
10^6	2^{20}	0.95	0.099	0.304
10^6	2^{21}	0.48	0.078	0.304
10^3	2^{20}	0.00095	0.046	0.0304
1	2^{21}	$4.77 \cdot 10^{-7}$	0.017	0.00304

$z_{\rm acc}$; the initial subhalo concentration, c; and three orbital parameters, as described in Section 2.3, i.e. the orbital energy parameter, $x_{\rm c}$, the orbit circularity, η, and the orbit inclination angle, θ, only relevant when including baryons.

We find in [20] that subhaloes passing $R_\odot$ typically have $x_{\rm c} = 1.2$ and $\eta = 0.3$ at accretion and adopt this pair as our fiducial choice. We summarize both the fiducial setting and the full suite in Table 1.

Finally, we note that our effective mass resolution will depend on the number of particles, N. In particular, $m_{\rm resol} = m_{\rm sub}/N$. We choose N such that we try to ensure convergence of results (see later below) for the particular set of parameters under consideration within our suite, sometimes increasing it significantly to fulfill this requirement from accretion time to present. Some of the adopted values in this work are listed in Table 2. In this same table, we also show the mean inter-particle distance, $d_{\rm ip}$ [23].

3. Results

In this section, we summarize the main findings in our analyses. We have mainly studied two relevant quantities: the bound mass fraction, $f_{\rm b}$, which corresponds to the fraction of the initial subhalo mass that remains bound at a given redshift, and the annihilation luminosity, L, which is defined as the integral of the subhalo density profile squared.

3.1 Bound mass fraction

The bound mass fraction comprises the information about how much mass the subhalo has lost when a certain amount of time has passed since its accretion. We define it as the fraction of mass

PoS(ICRC2023)004

that remains bound at time t with respect to the initial subhalo mass [11]:

$$f_{\rm b} = \frac{M(t)}{M_{200,\rm sub}}, \tag{5}$$

where $M(t)$ is the bound mass of the subhalo at time t, and $M_{200,\rm sub} = M(< r_{200,\rm sub}) = m_{\rm sub}$ is the initial virial mass of the subhalo. This virial radius will not be a good parameter to define the subhalo after accretion, since the mass at the outskirts will be eventually lost and its profile will be consequently truncated.

This quantity allows us to elucidate if the subhalo has been disrupted or if it survives after several orbits. We study $f_{\rm b}$ for the cases in which the host is made of DM alone as well as the one in which baryons are also included. These cases are detailed, respectively, in the next Sections 3.1.1 and 3.1.2. Furthermore, we study the values of $f_{\rm b}$ that can be trusted in our analyses via the definition of strict convergence criteria in either case, which are nailed down in [20].

3.1.1 Non-baryonic case

Most significant changes occur at the pericentre, when a larger fraction of material from the subhalo is stripped by the host. In Fig. 1, we show $f_{\rm b}$ as a function of the scale factor, $a = 1/(1+z)$, for different subhalo configurations. In each of them, we vary a parameter among those defining our fiducial setup specified in Table 1. In particular, in the upper panels of Fig. 1, we show the evolution of $f_{\rm b}$ for different concentrations and circularities, respectively. From these panels one can see that less concentrated subhaloes at accretion lose mass more quickly, which agrees with the expectations. Also, more radial orbits, i.e. those with smaller η, imply a larger mass loss. Note that we are comparing different eccentricities here while fixing $x_{\rm c}$. Therefore, our orbits with higher eccentricities have smaller pericentres and experience a stronger tidal field. In the lower left panel of Fig. 1 different orbital energy parameter values are displayed. In this case, a smaller $x_{\rm c}$ leads to a larger number of orbits in the same time interval and, thus, to a greater mass loss as well. Finally, the lower right panel shows examples for different accretion redshifts, and we can see that a larger $z_{\rm acc}$ has also the effect of inducing more mass loss: the subhalo completed more orbits and it initially had a smaller pericentre because the host halo was smaller at earlier cosmic epochs. Indeed, subhaloes accreted at different times landed on different orbits and later-accreted subhaloes have spent less time within the host. We use $N = 2^{18}$ particles in most cases, increasing this number up to $N = 2^{21}$ whenever needed.

A general picture of $f_{\rm b}$ results at $z = 0$ in the non-baryonic case can be seen in the upper left panel of Fig. 3. In this plot, we fix $x_{\rm c} = 1.2$ and $z_{\rm acc} = 2$ and vary both the concentration and η parameters. The summary is that subhaloes lose less mass when any of these two parameters is larger. These results are expected to be scale-free when the subhalo mass is small enough. More specifically, results will be identical for ratios $M_{200,\rm host}/m_{\rm sub} \gtrsim 10^3$, since self-friction becomes negligible [13].

3.1.2 Baryonic case

Recent hydrodynamical simulations have shown a significant decrease of the number of subhaloes when baryons are taken into account [15–17, 24]. However, this could still be due to numerical artifacts related to insufficient mass and/or force resolution [11, 12]. In our work, we

PoS(ICRC2023)004

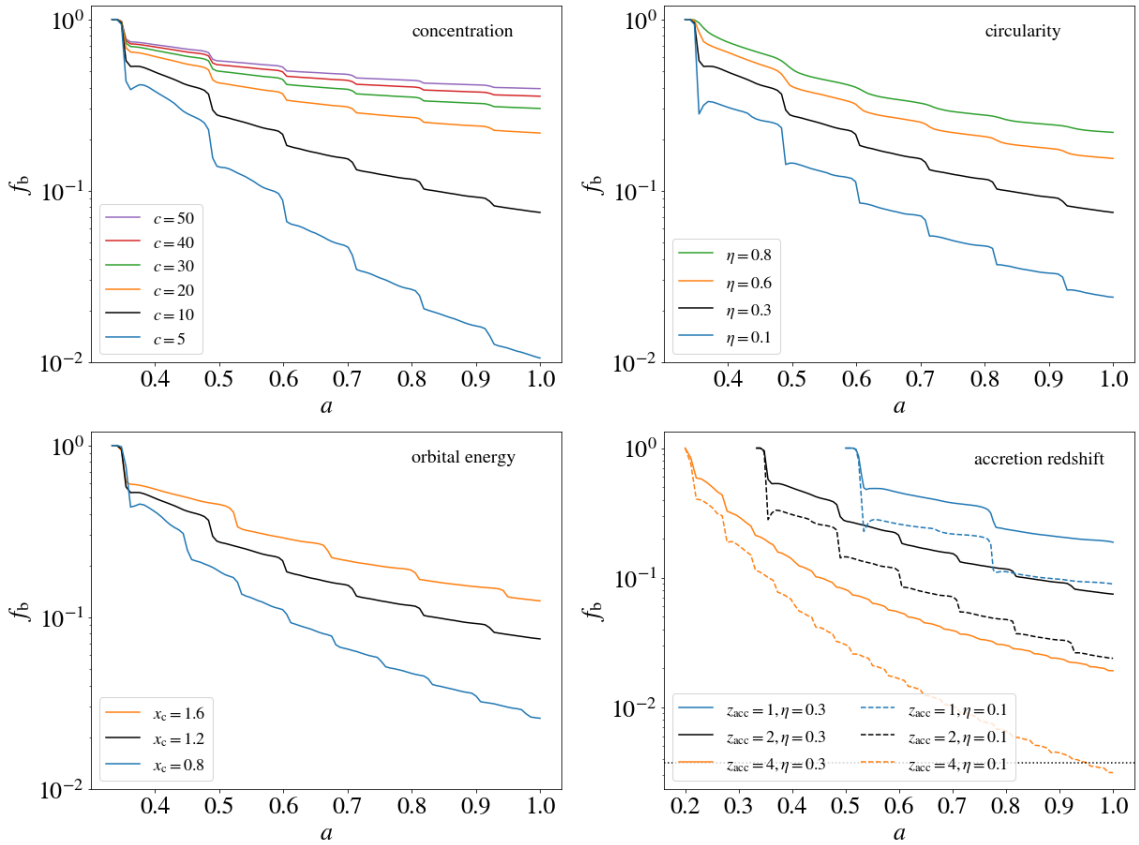

Figure 1: Bound mass fraction, f_b, as a function of $a = 1/(1+z)$ for different subhalo configurations. Each of them corresponds to a case in which we vary one parameter among those representing our fiducial setup in Table 1. The latter is depicted as a solid black line in all panels for reference. Upper left panel: Different initial subhalo concentrations (c). Upper right panel: Different initial circularities (η). Lower left panel: Different orbital energies (x_c). Lower right panel: Different accretion redshifts (z_{acc}) using two different circularity values. The black horizontal dotted line sets the convergence value for f_b. When it does not appear, this value is below the chosen y-axis lower limit. Note that f_b is always well above except in the lower right panel, for which no convergence is achieved at present time for the case of $z_{acc} = 4, \eta = 0.1$.

want to give an answer to this ongoing debate by performing a variety of simulations including the baryonic component of a MW-size halo as well. Therefore, in order to obtain more realistic simulations we now add baryonic material to the host potential.

In Fig. 2, we compare the impact that adding baryons or not to the host potential has on the bound mass fraction. We adopt an inclination angle of 45 degrees in this example as an intermediate choice. As it can be seen, the presence of baryonic material can have a huge impact on the subhalo depletion, especially when the pericentre of the orbit is smaller (e.g. decreasing η while fixing x_c). This typically leads to a much smaller f_b for the same time after accretion when compared to the non-baryonic case. Indeed, Fig. 2 shows that some non-baryonic runs with smaller η but larger c can lead to comparatively less mass loss, while this is not necessarily the case when baryons are included.

PoS(ICRC2023)004

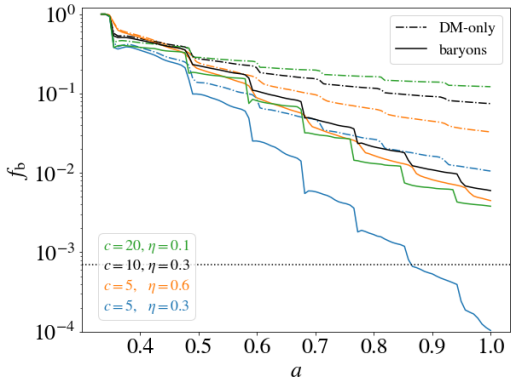

Figure 2: Comparison between adding baryons to the host halo potential or having only DM, for both different concentration and orbital circularity values. The fiducial setup of Table 1 is shown as a black line. Non-baryonic runs are depicted as dash-dotted lines while baryonic ones are in solid. The black dotted horizontal line corresponds to the convergence limit. In all cases, we set $x_c = 1.2$, $z_{acc} = 2$ and $m_{sub} = 10^6 M_\odot$. When baryons are included, the inclination angle is 45 deg.

A general picture of f_b results at $z = 0$ for the runs including baryons can be seen in the middle left panel of Fig. 3. In this plot, we fix the inclination angle of the subhalo orbit to 45 degrees, adopt $x_c = 1.2$ and $z_{acc} = 2$, and vary both the concentration and η parameters. Again, we conclude that subhaloes lose less mass when any of these two last parameters is larger. We note that we cannot achieve numerical convergence for a few cases in our grid[2], although we do for most of them. An example of the latter can be actually seen as the blue solid line in Fig. 2 as well. The lower left panel of Fig. 3 shows the ratio between baryonic and DM-only runs, and confirms again the larger impact of baryons, especially for subhaloes in more radial orbits.

3.2 DM annihilation luminosity

Studying the annihilation luminosity of galactic subhaloes is essential to understand their potential as targets for gamma ray searches [4]. For instance, current DM constraints obtained from the scrutiny of unidentified gamma-ray sources in search of potential subhaloes with no visible counterparts depend, in the first place, on the number of detectable subhaloes predicted from a combination of simulations and instrumental sensitivity [e.g. 18]. More specifically, these DM constraints would be overly optimistic if a significant fraction of subhaloes in the solar vicinity disrupt or lose a significant fraction of their luminosity. Having more resilient subhaloes than those in current simulations would also impact the mentioned DM constraints, this time in the opposite way. Thus, for these studies it is important to have robust predictions of the number of subhaloes. In particular, knowing both the precise abundance and radial distribution of the subhalo population within a MW-like host would be of utmost importance, not only from a purely cosmological perspective and for current DM constraints, but also e.g. to understand the role of subhaloes for the so-called subhalo annihilation boost [25, 26].

[2]We have tried to improve the convergence using different values of N, up to 2^{21}, but did not succeed. We note though that enlarging N even more drastically should allow to reach a convergent run in the end for most cases; however, the computational resources needed to do so were too expensive.

PoS(ICRC2023)004

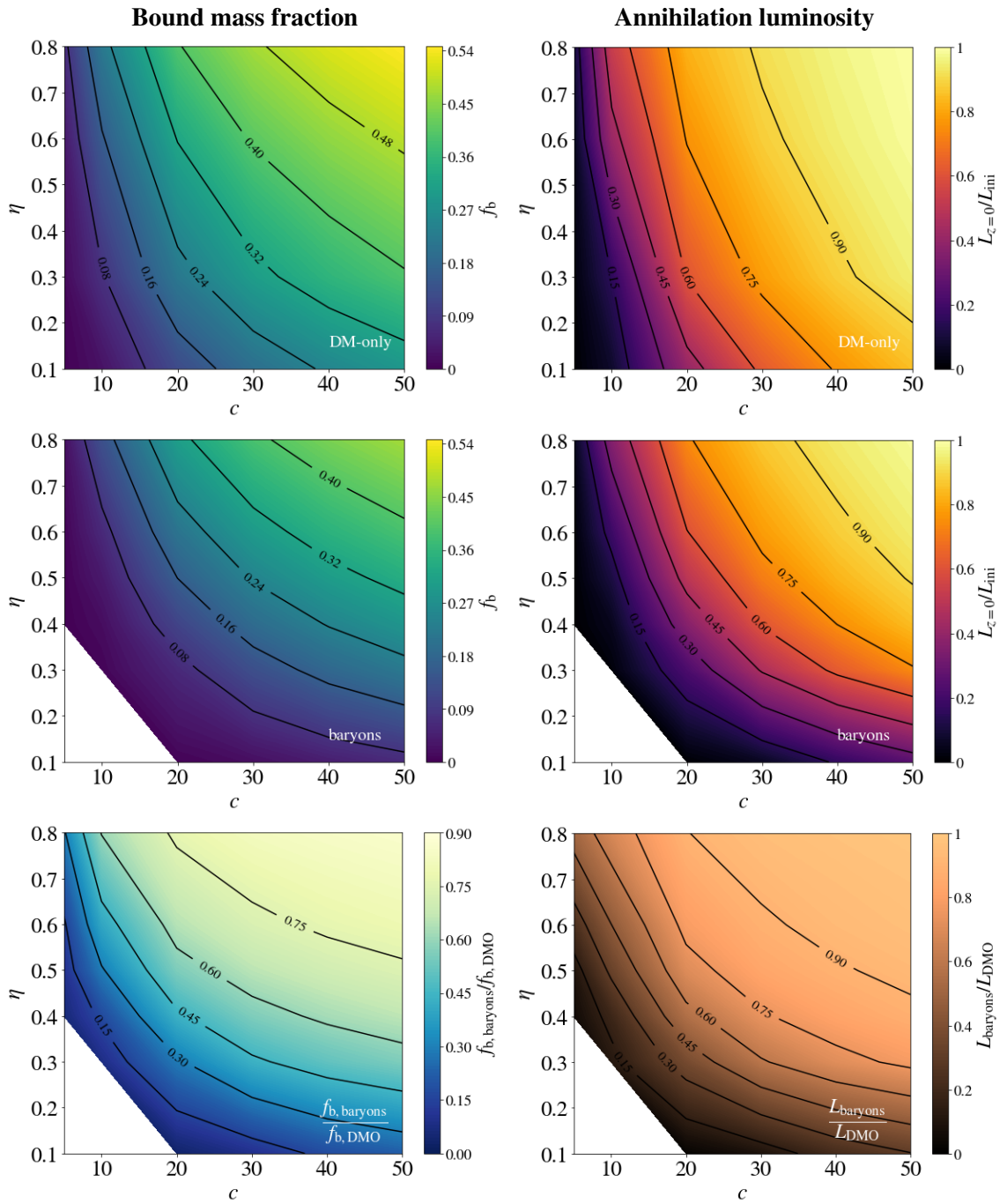

Figure 3: Left: Bound mass fraction, f_b, at present time for different initial subhalo concentrations and circularities in the non-baryonic case (top) and in case of including baryons (middle). The ratio between the two previous panels, i.e. $f_{b,baryons}/f_{b,DMO}$ at $z = 0$, is shown in the bottom panel. Right: Annihilation luminosity results at $z = 0$ varying both the concentration and η parameters, both for the case of excluding baryons (top panel) and with baryons included (middle). The bottom panel shows the ratio between the two previous panels, i.e. $L_{baryons}/L_{DMO}$ at $z = 0$. We adopt a one-million-solar-mass subhalo, with $x_c = 1.2$ and $z_{acc} = 2$ in all cases, and fix the inclination angle of the subhalo orbit to 45 degrees in the case of baryons. Non-converged runs are not shown and are the cause of the blank regions in these plots.

PoS(ICRC2023)004

The way to compute the subhalo luminosity is via the radial density profile $\rho(r)$; more specifically, we define the annihilation luminosity in our study as the integration of the DM density profile squared: $L = \int_V \rho^2(r)\, dV$. The fraction of this annihilation luminosity that reaches the Earth and we can potentially measure with our telescopes is the annihilation flux. We note, however, that the latter cannot be predicted without knowing the exact distance between the subhalo and us.

The lack of numerical resolution in the innermost part of the subhalo together with the effect of particle relaxation makes the study of the annihilation luminosity a difficult task. To solve this problem, we reconstruct the inner cusp in each snapshot in a semi-analytical way. Full details of this cusp reconstruction can be found in [20].

In Fig. 4, we show the evolution of the annihilation luminosity normalized to its initial value at accretion, $L/L_{\rm ini}$, as a function of the scale factor, $a = 1/(1+z)$, for different subhalo configurations. In particular, in the left panel we show the evolution for different concentrations, concluding that less concentrated subhaloes at accretion get reduced to a smaller fraction of their initial luminosity (by e.g. a factor ~ 4 in the fiducial case), which is in tune with expectations. A comparison between runs without and with baryons is shown in the right panel. Notice again that η becomes relevant when baryons are included, since a small value induces a greater change in the luminosity.

A general picture of annihilation luminosity results at $z = 0$ varying both the concentration and η parameters can be seen in Fig. 3, both for the case of excluding baryons (top right panel) and with baryons included (middle right). We adopt $x_{\rm c} = 1.2$ and $z_{\rm acc} = 2$ in all cases, and fix the inclination angle of the subhalo orbit to 45 degrees in the case of baryons. As in the case of $f_{\rm b}$, we do not reach numerical convergence for a few cases in our grid, although we do for most of them. For our fiducial subhaloes (Table 1) there is always a significant reduction of luminosity, the subhalo retaining about 15% and 2% of its initial luminosity in the non-baryonic and baryonic cases, respectively. More in general, it can be seen that the concentration is the most relevant parameter when baryons are not considered, the subhalo not losing a significant luminosity fraction when c is large enough, while also η plays a major role when baryons are added to the game. More specifically, baryons have a large impact on the annihilation luminosity when the orbits are more radial (smaller η) since the subhalo gets closer to the host halo centre, where baryons are mostly located, thus enhancing the disruption. This is more clearly visible in the bottom right panel of the same Fig. 3, which shows the ratio between annihilation luminosities found at $z = 0$ in the baryonic and DM-only cases.

4. Discussion

In this section we try to simplify the parameter space of tidal stripping by summarizing it into a single parameter. First, in Section 4.1, we show that most dependence of the mass loss on orbital parameters can be summarized through its dependence on the pericentre radius of the orbit. As a further simplification, we show in Section 4.2 that baryonic and DM-only cases follow the same relation when the pericentre tidal field is considered as the primary parameter instead and further, that also the concentration dependence can be explained by defining a single effective tidal field parameter that takes into account the structure-tide degeneracy [14].

PoS(ICRC2023)004

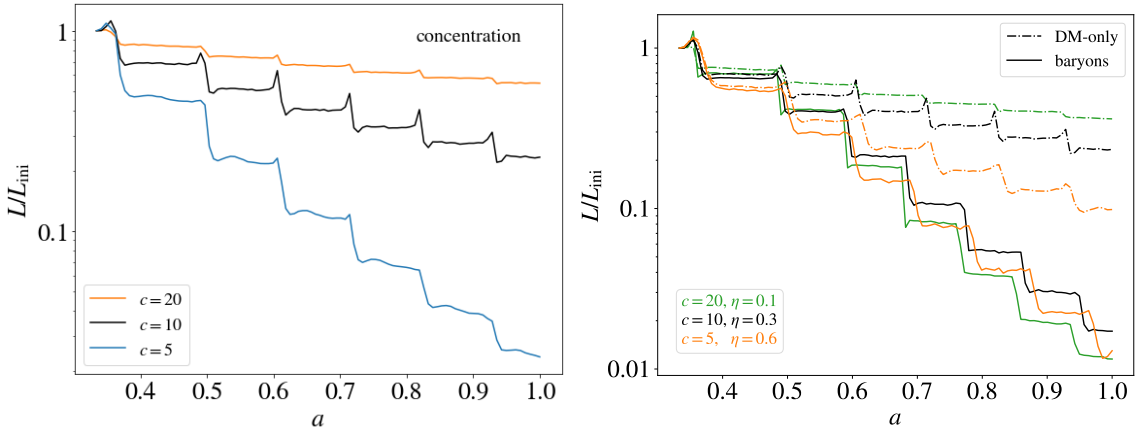

Figure 4: Evolution of the annihilation luminosity normalized to its initial value at accretion, $L/L_{\rm ini}$, as a function of the scale factor, $a = 1/(1+z)$, for different initial subhalo concentrations (left) and comparison for runs with and without baryons (right).

Table 3: Best-fit parameters and uncertainties for the power law function relating the pericentres with $f_{\rm b}$, given by Eq. (6), and for the function relating the pericentres and $L_{z=0}/L_{\rm ini}$, described in equation (7), both for the cases without and with baryons. These fits are for a particular value of concentrations, namely $c = 10$, and are shown in Fig. 5 together with the data used to perform the fits. See Section 4.1 for details.

	without baryons	with baryons
m	1.07 ± 0.07	1.77 ± 0.16
$\log_{10} e$	0.25 ± 0.10	0.58 ± 0.17
n	1.43 ± 0.04	3.0 ± 0.4
d	1.3 ± 0.1	5 ± 1

4.1 On the pericentres

Good approximate predictions can still be obtained only through knowledge of a small subset of the parameters. Here, we try to understand what the single most predictive parameter for estimating the mass loss is. First, we investigate the orbital pericentre as a candidate.

In the left panel of Fig. 5 we show $f_{\rm b}$ at present time as a function of the pericentre of the orbit[3] for different orbital parameters and accretion redshifts, We adopt $c = 10$ in all cases. Our results show that these points are roughly aligned in log-log space:

$$f_{\rm b} = e(r_{\rm peri}/r_{200,\rm host})^m, \tag{6}$$

where $r_{\rm peri}/r_{200,\rm host}$ is the value of the pericentre in each case, in terms of the virial radius of the host at $z = 0$. Our best fit parameters for those data are listed in Table 3. The corresponding fits are also shown in the left panel of Fig. 5 together with their respective scatter.

[3]To be precise, among all pericentres since accretion, we select the one with the minimum distance to the host halo centre. Some small variations are indeed observed among pericentres in the same run, of the order of 10-20%.

PoS(ICRC2023)004

As expected, a smaller pericentre induces a larger mass loss in general. This effect is much greater when baryons are taken into account, since they strongly enhance the tidal field in the centre of the host. The scatter suggests that, even if the pericentric distance is the driving effect in the mass loss, there are other effects also present in the process. Notice that both the non-baryonic and baryonic cases agree when the pericentre is sufficiently large; see [20] for details.

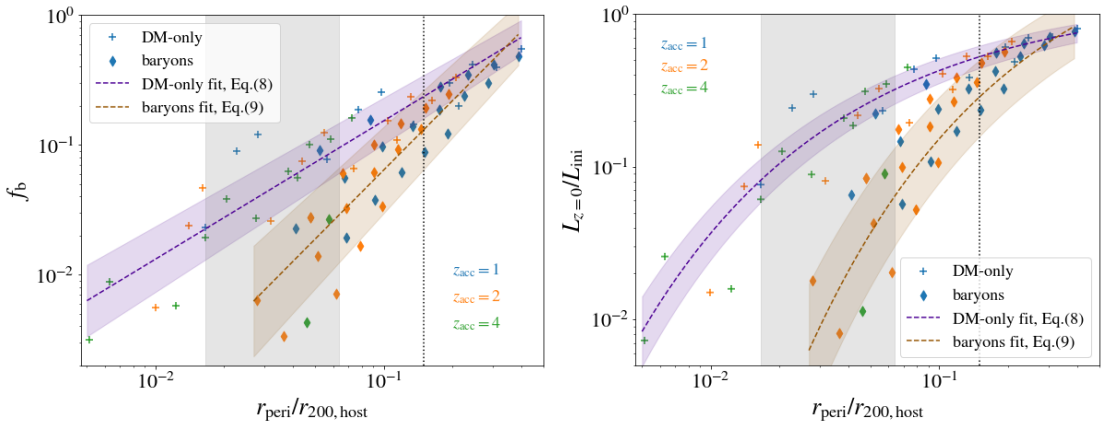

Figure 5: Left: Bound mass fraction at present time as a function of the subhalo pericentric distance in units of the host virial radius at $z = 0$, $r_{peri}/r_{200,host}$, as found in different runs with an initial subhalo concentration $c = 10$. Right: Annihilation luminosity at present time, normalized to the initial one, as a function of the subhalo pericentric distance in units of the host virial radius, $r_{peri}/r_{200,host}$, as found in different runs with an initial subhalo concentration $c = 10$ and varying the orbital parameters and accretion redshifts. In both panels, dashed purple and brown lines correspond to fits to Eq. (6) and (7) using the best-fit parameters collected in Table 3 for both the cases without and with baryons, respectively. The grey area corresponds to the solar vicinity, defined as the galactocentric region within 8.5 ± 5 kpc. The black dotted line shows the radius at which the baryonic tidal field is comparable to the DM halo one; see discussion in Section 4.1 and [20].

We have done the same analysis for the annihilation luminosity. The right panel of Fig. 5 shows its value at present time normalized to the initial one versus the pericentre of the orbit. We used the same runs that were used for the left panel of the same figure. From this exercise we can estimate the luminosity loss of subhaloes in the solar vicinity, depicted as a grey shaded region in the right panel of Fig. 5. In particular, if we only consider DM inside the host, subhaloes lose between 70 and 90 per cent of their initial L. When we add baryons, this percentage can increase up to 99%.

We did not find a power-law behaviour in this case. We propose the following fitting function:

$$L_{z=0}/L_{ini}(r) = d \cdot n^{-1/\sqrt{r}}, \tag{7}$$

Our best-fit parameters are also listed in Table 3. In this case, we observe again that both DM-only and baryonic results converge for large pericentric distances.

While it is intriguing to see that mass loss and luminosity follow simple relations as a function of the pericentre radius, we want to emphasize here that the obtained relations will additionally depend on the initial concentration of the subhalo and on parameters that modify the host potential.

PoS(ICRC2023)004

4.2 Mass loss and the pericentre tidal field

As we have seen in Fig. 5, the pericentre versus mass loss relation is different for host potentials that consider baryons and those which do not. This makes sense since tidal fields are much stronger in the host centre in the baryonic cases than in the DM-only case.

In [14], we have proposed that both of these cases may be unified into a single relation if we consider their pericentre tidal fields instead of their radii as the important parameters. Additionally, we have proposed in [14] that the concentration dependence of the tidal stripping problem should additionally disappear if we measure tidal fields in units of the scale tide $\lambda_{\rm s}$ and masses in units of the scale mass $M_{\rm s}$.

In [14], we have developed a simple model that describes NFW haloes that are exposed to a tidal field, the latter increasing so slowly that the halo responds adiabatically. In the adiabatic limit (and assuming an isotropic tidal field), $M_{\rm b}/M_{\rm s}$, where $M_{\rm b}$ is the remaining mass in such limit, is exactly only a function of the effective tidal field, $\lambda/\lambda_{\rm s}$. Now, in realistic setups many additional dependencies exist, but we would still expect that at first order most of the host potential dependence and most of the concentration dependence should disappear if results are presented in this way. Here we want to test this expectation.

We infer the maximum eigenvalue among all of the timesteps and we define this value as the pericentre tidal field, $\lambda_{\rm peri}$. Using the maximum of the tidal field as $\lambda_{\rm peri}$ has the advantage that it is always well defined even in cases of anisotropic or evolving host potentials, etc.

We show the mass loss $M/M_{\rm s}$ as a function of $\lambda_{\rm peri}/\lambda_{\rm s}$ in the left panel of Fig. 6, where we have combined runs with different configurations. Strikingly, the cases with and without baryons follow the same relation when shown in this manner. This shows that the largest encountered tidal field is indeed the single most important parameter for understanding tidal mass loss. Of course, there is a sizeable scatter in the relation, which shows that secondary dependencies exist. Yet, the relation is now considerably tighter than the one shown in the left panel of Fig. 5. In the same left panel of Fig. 6, we show a line corresponding to the adiabatic limit of [14], which represents the absolute maximum expected mass loss in this parameter space. We note that our measured values here still lie quite far from the adiabatic limit. This is expected, as these subhaloes have orbited for much shorter times than what is necessary to reach the mentioned limit.

In the right panel of Fig. 6 we show the mass loss as a function of the effective tide and concentration. When presented in these reduced units, the concentration dependence indeed disappears, i.e. the iso-contours in this plot are approximately horizontal. This shows that much of the parameter space of the tidal mass loss problem can be simplified and generalized. We call this phenomenon the "structure-tide" degeneracy and we explain in [14] how this arises from the invariance of the Vlasov-Poisson system to time-rescalings.

5. Conclusions

Cosmological N-body simulations are computationally expensive and they are prone to both mass and spatial resolution limits, which makes it very difficult to properly resolve subhaloes and follow their evolution within their hosts. In contrast, employing an analytical prescription when modelling the host halo potential gives plenty of room to simulate a subhalo and to track its evolution with great accuracy and numerical resolution.

PoS(ICRC2023)004

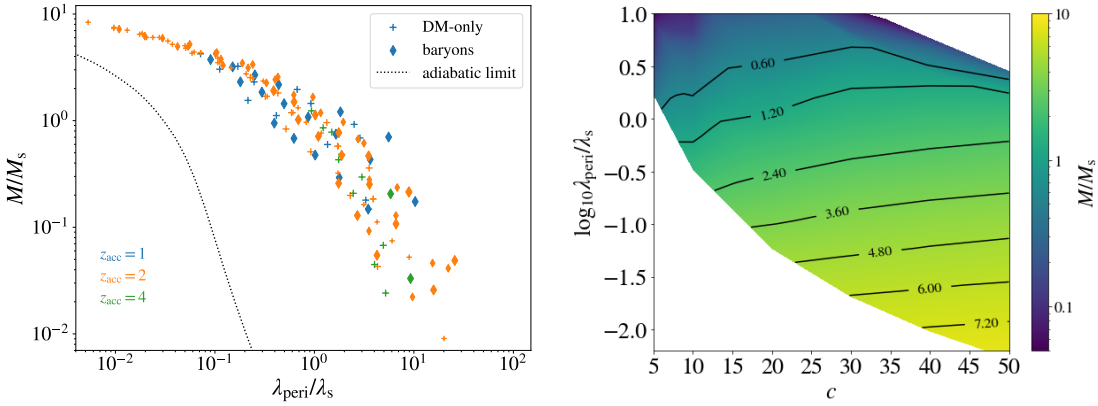

Figure 6: Left: Subhalo mass at present divided by the initial scale mass, as a function of the effective tide, λ_s, for different subhalo concentrations (for $z_{acc} = 2$), redshifts (for $c = 10$) and orbital parameters, both with (diamonds) and without (plus signs) baryons. The dotted line is the adiabatic limit of [14]. Right: Remaining subhalo mass at present time divided by the scale mass, for different concentrations and effective tides at the pericentre.

This work makes use of DASH, a code specifically designed to perform this task with unprecedented accuracy, reaching solar-mass and sub-parsec resolution in our simulations, implementing a few, important novelties with respect to the original version in [13].

We have studied the evolution of subhaloes in a MW potential, exploring different subhalo configurations, adopting a fiducial set of parameters as the representative case, but also varying one or some of these parameters to understand the role of each of them in the evolution of the subhalo. We have focused on studying two quantities particularly relevant for our purposes, the bound mass fraction and the DM annihilation luminosity, and performed several checks. Our main findings can be summarized as follows:

- ⋆ Contrary to [16, 27], we find that subhaloes do survive in the innermost 15 kpc of our galaxy, although they typically lose more than 90% of their initial masses.
- ⋆ Subhaloes with lower concentrations and subhaloes on orbits with smaller pericentric distances are more depleted. Similarly, subhaloes accreted earlier or with lower orbital energies have smaller orbits and have lost more mass at $z = 0$. Including baryonic material in the host induces a significantly larger mass loss in most cases as well.
- ⋆ Subhaloes orbiting a DM-only halo with a pericentre in the solar vicinity have lost 70-90% of their initial annihilation luminosity at $z = 0$ for DM-only runs and up to 99% when baryons are included in the host. We emphasize that our results are virtually independent of subhalo mass for subhaloes lighter than 10^8 $M_\odot$.
- ⋆ We have found new ways of summarizing the most important dependencies on the parameter space into a single parameter. Firstly, we have found a first order simplification using the pericentre radius. We have found simple powerlaw relations for a $c = 10$ subhalo that orbits in a Milky-Way like host –with different relations for baryonic and DM-only cases.

PoS(ICRC2023)004

- ⋆ Motivated by the analytical arguments of [14], we have additionally found that the problem can be further simplified, by summarizing the concentration and host-potential dependence into the single parameter λ/λ_s –the effective tidal field at pericentre. Both the host-potential dependence (e.g. baryons versus DM-only) and the concentration dependence are captured.

Studying subhalo survival is crucial to elucidate the role of small subhaloes in indirect DM searches, which was one of the key motivations to perform this work. Among potential future applications of our work we can mention, for instance, a more refined calculation of the so-called subhalo boost factor to annihilation signals, more robust constraints on DM, and the optimization of DM search observation strategies for spatially extended DM targets. Regarding the boost in particular, we can already anticipate that the annihilation signal will be boosted by these surviving subhaloes in the solar vicinity [e.g. 25]. Further work is needed though to accurately compute this factor, as we expect it to be not as high as most of these works may suggest.

This work is still ongoing. In the near future, we will take a closer look at the evolution of the subhalo concentration with time, as well as the impact of the latter for indirect DM searches. We would also like to understand the impact of our findings on both the radial distribution and mass function of the MW subhalo population. Besides, we are considering running more massive simulations with higher resolution, which will allow to track $f_{\rm b}$ for more extreme c cases, as well as calculating the annihilation luminosity with higher confidence.

References

[1] G. Bertone and D. Hooper, *History of dark matter*, *Rev. Mod. Phys.* **90** (2018) 045002 [1605.04909].

[2] N. Aghanim, Y. Akrami, M. Ashdown, J. Aumont, C. Baccigalupi, M. Ballardini et al., *Planck 2018 results. VI. Cosmological parameters*, *AAP* **641** (2020) A6 [1807.06209].

[3] G. Bertone and D. Merritt, *Dark Matter Dynamics and Indirect Detection*, *Modern Physics Letters A* **20** (2005) 1021 [astro-ph/0504422].

[4] M. Ackermann, A. Albert, L. Baldini, J. Ballet, G. Barbiellini, D. Bastieri et al., *Search for Dark Matter Satellites Using Fermi-LAT*, *APJ* **747** (2012) 121 [1201.2691].

[5] T.A. Porter, R.P. Johnson and P.W. Graham, *Dark Matter Searches with Astroparticle Data*, *ARA&A* **49** (2011) 155 [1104.2836].

[6] J. Zavala and C.S. Frenk, *Dark Matter Haloes and Subhaloes*, *Galaxies* **7** (2019) 81 [1907.11775].

[7] J. Diemand, M. Kuhlen and P. Madau, *Formation and Evolution of Galaxy Dark Matter Halos and Their Substructure*, *Astrophys. J.* **667** (2007) 859.

[8] M. Vogelsberger, F. Marinacci, P. Torrey and E. Puchwein, *Cosmological simulations of galaxy formation*, *Nature Reviews Physics* **2** (2020) 42 [1909.07976].

[9] R.E. Angulo and O. Hahn, *Large-scale dark matter simulations*, *Living Reviews in Computational Astrophysics* **8** (2022) 1 [2112.05165].

[10] R.E. Angulo, C.M. Baugh, C.S. Frenk and C.G. Lacey, *Extending the halo mass resolution of N-body simulations*, *MNRAS* **442** (2014) 3256 [1310.3880].

PoS(ICRC2023)004

[11] F.C. van den Bosch, G. Ogiya, O. Hahn and A. Burkert, *Disruption of dark matter substructure: fact or fiction?*, *MNRAS* **474** (2018) 3043 [1711.05276].

[12] F.C. van den Bosch and G. Ogiya, *Dark matter substructure in numerical simulations: a tale of discreteness noise, runaway instabilities, and artificial disruption*, *MNRAS* **475** (2018) 4066 [1801.05427].

[13] G. Ogiya, F.C. van den Bosch, O. Hahn, S.B. Green, T.B. Miller and A. Burkert, *DASH: a library of dynamical subhalo evolution*, *MNRAS* **485** (2019) 189 [1901.08601].

[14] J. Stücker, G. Ogiya, R.E. Angulo, A. Aguirre-Santaella and M.A. Sánchez-Conde, *Tidal Stripping in the Adiabatic Limit*, *arXiv e-prints* (2022) arXiv:2207.00604 [2207.00604].

[15] S. Garrison-Kimmel, A. Wetzel, J.S. Bullock, P.F. Hopkins, M. Boylan-Kolchin, C.-A. Faucher-Giguère et al., *Not so lumpy after all: modelling the depletion of dark matter subhaloes by Milky Way-like galaxies*, *MNRAS* **471** (2017) 1709 [1701.03792].

[16] T. Kelley, J.S. Bullock, S. Garrison-Kimmel, M. Boylan-Kolchin, M.S. Pawlowski and A.S. Graus, *Phat ELVIS: The inevitable effect of the Milky Way's disc on its dark matter subhaloes*, *MNRAS* **487** (2019) 4409 [1811.12413].

[17] R.J.J. Grand, F. Marinacci, R. Pakmor, C.M. Simpson, A.J. Kelly, F.A. Gómez et al., *Determining the full satellite population of a Milky Way-mass halo in a highly resolved cosmological hydrodynamic simulation*, *MNRAS* **507** (2021) 4953 [2105.04560].

[18] J. Coronado-Blázquez, M.A. Sánchez-Conde, A. Domínguez, A. Aguirre-Santaella, M.D. Mauro, N. Mirabal et al., *Unidentified gamma-ray sources as targets for indirect dark matter detection with the Fermi-Large Area Telescope*, *JCAP* **2019** (2019) 020.

[19] J.F. Navarro, C.S. Frenk and S.D.M. White, *A Universal Density Profile from Hierarchical Clustering*, *APJ* **490** (1997) 493 [astro-ph/9611107].

[20] A. Aguirre-Santaella, M.A. Sánchez-Conde, G. Ogiya, J. Stücker and R.E. Angulo, *Shedding light on low-mass subhalo survival and annihilation luminosity with numerical simulations*, *MNRAS* **518** (2023) 93 [2207.08652].

[21] J. Barnes and P. Hut, *A hierarchical O(N log N) force-calculation algorithm*, *Nature* **324** (1986) 446.

[22] G. Ogiya, M. Mori, Y. Miki, T. Boku and N. Nakasato, *Studying the core-cusp problem in cold dark matter halos using N-body simulations on GPU clusters*, in *Journal of Physics Conference Series*, vol. 454 of *Journal of Physics Conference Series*, p. 012014, Aug., 2013, DOI.

[23] A.L. Melott, S.F. Shandarin, R.J. Splinter and Y. Suto, *Demonstrating Discreteness and Collision Error in Cosmological N-Body Simulations of Dark Matter Gravitational Clustering*, *APJl* **479** (1997) L79 [astro-ph/9609152].

[24] S.B. Green, F.C. van den Bosch and F. Jiang, *SatGen - II. Assessing the impact of a disc potential on subhalo populations*, *MNRAS* **509** (2022) 2624 [2110.13044].

[25] A. Moliné, M.A. Sánchez-Conde, S. Palomares-Ruiz and F. Prada, *Characterization of subhalo structural properties and implications for dark matter annihilation signals*, *Monthly Notices of the Royal Astronomical Society* (2017) stx026.

[26] M.A. Sánchez-Conde and M. Doro, *Special Issue 'The Role of Halo Substructure in Gamma-Ray Dark Matter Searches'* (July, 2020), 10.3390/books978-3-03936-045-1, [2007.01747].

[27] R.J.J. Grand and S.D.M. White, *Baryonic effects on the detectability of annihilation radiation from dark matter subhaloes around the Milky Way*, *MNRAS* **501** (2021) 3558 [2012.07846].

PoS(ICRC2023)004